In-Situ QAM-based Power Line Communication for Large-Scale Intelligent Battery Management

Mahyar J. Koshkouei* ⓘ, Erik Kampert ⓘ, Andrew D. Moore ⓘ, and Matthew D. Higgins ⓘ

WMG, University of Warwick, Coventry, UK

mahyar.koshkouei@warwick.ac.uk

Abstract—The use of power line communication (PLC) within a large-scale battery will allow for smart cells to communicate within a decentralised system, with an external battery management system (BMS), and also with an external smart grid network. By using PLC, the smart battery is further enhanced by allowing the BMS real-time access to in-situ cell sensor data, without the need of an additional wire harness within the battery. This paper presents experimental studies of a PLC system on four distinct lithium-ion battery pack configurations, in order to determine its suitability and limitations for large-scale energy storage systems such as for use in smart grids, battery electric vehicles, and robotic systems. Quadrature amplitude modulation (QAM) is tested up to 1024-QAM for its benefits in high bit rate communication. Recommendations on the parameters of this PLC system based upon experimental results are presented.

Index Terms—Smart Grid, Power Line Communication, Smart Cells, Intelligent Vehicles, Energy Storage Communication, Quadrature Amplitude Modulation, Battery Management.

I. INTRODUCTION

The advance of intelligent battery electric vehicles (BEVs), focusing on eco-driving strategies, is expected to provide a safe and energy-efficient mode of travel. As the number of BEVs increases, current research addresses their limited battery energy, thereby focusing on energy management and optimisation [1]. However, BEVs still remain a minority in the overall vehicle market share in part due to their relative disadvantages that include limited driving range on a single charge, long charging time, and perceived comparative high purchase and running costs [2]. Further developments in technologies and techniques are necessary to tackle these limitations, hence an ongoing interest and focus of the research community exists for these themes.

The parameters and characteristics of the energy storage system within the BEV can directly influence the driving range and the charging time. Consequently, the lithium-ion (Li-ion) cell is typically used within such energy storage systems, as it offers high capacity, energy density, power density and lack of memory effects over other battery chemistries, such as nickel-metal hydride and lead acid [3]. Nevertheless, the use of Li-ion cells is limited by its sensitivity to ambient and internal temperatures, working voltages, and charging/discharging current

rates. These constraints mitigate performance regressions and lifetime reductions, since further stress might otherwise cause thermal runaway, fire or explosion [4].

A battery management system (BMS) is used to monitor and control the use of cells within a battery pack. Its features include cell balancing and charge rate control, which improve the safety and performance of Li-ion cells within a battery pack [3]. This performance involves charge/discharge rates and the regulation of their energy consumption for higher capacity. Further improvements can be made by utilising instrumented cells, which are, among others, able to perform in-situ temperature sensing within Li-ion cells [5]. However, the use of instrumented cells is limited by the requirement for a wired connection to the external system, including the BMS. If each cell within a large battery pack is instrumented, the number of wires required to connect them to the BMS would increase the complexity and weight of the battery pack, thereby reducing its overall power density [6].

Established literature demonstrates the use of smart cells, which utilise an embedded system to perform intelligent operations without an external system. Such smart cells include the cell management system (CMS) which is able to monitor sensors within a single cell [7], and utilise this data to perform further safety and performance tasks, including local temperature regulation [8] and cell balancing [9], that are not possible with a BMS alone. These techniques allow for improvements in energy storage efficiency and performance, and may result in further reductions of the charging time [10] as well as increase in the travelling distance for BEVs [11]. The CMS makes each smart cell work independently of one another, and therefore does not require a wired link to a BMS. However, since these CMS smart cells work independently, their capability in improving safety and performance is limited due to their assumptions that must be made for other cells within the same battery pack.

In order to remove this limitation of the CMS, a communication system can be used to transmit local sensor data from the smart cell to an external BMS, to other smart cells when used within a decentralised network, or to an external smart grid. The BMS, which will receive sensor data from all smart cells, will then be able to make improved safety and performance decisions by removing the need to make assumptions on the status of other cells within the battery pack. These improvements include fault detection and performance management of each specific smart cell. Such a communication

system must not require any additional wire harness in order to mitigate any losses to power density. Therefore, power line communication (PLC) is considered for use within this system, in which the power network is also used as a communication channel. This allows for existing bus bars within BEV battery packs to be used for data communication. A circuit based model of 13 prismatic Li-ion cells has been simulated for the purpose of investigating their channel characteristics with PLC for frequencies of 1 MHz to 100 MHz [12]. The performance of an in-situ Li-ion QAM-based PLC system was evaluated within a simulated environment of a BEV driving under a real-world profile [13]. A smart system of instrumented 21700-model Li-ion cells utilising PLC for internal temperature, voltage, and current sensing was demonstrated in [14]. The changes in the performance of in-situ Li-ion PLC with state of charge has been presented in [15]. An in-situ communication network may be exploited by extending PLC from within the energy storage system through to an external smart grid. This thereby creates the potential to enhance renewable energy resource management and remote monitoring of battery health [16].

This paper presents measurements of PLC within various configurations of Li-ion battery packs, evaluates limitations within the communication system, and makes recommendations on the parameters of such a PLC system within a large-scale battery pack as used within a BEV for intelligent battery management. The use of quadrature amplitude modulation (QAM) is tested within this system, and is evaluated for its effectiveness in noise rejection and data rate within the target system. QAM allows for a more efficient use of the communication channel by mapping a series of bits to a symbol on a constellation map.

The key contributions of this paper are:

1) Analysis and comparisons of the communication performance of QAM with PLC on 18650-model Li-ion cells in smart battery pack configurations of a single cell, two cells in series, two cells in parallel, and two cells in series and two in parallel, testing carrier frequencies in the range from 10 MHz to 200 MHz.
2) Recommendations of communication parameters based upon empirical evidence.

II. EXPERIMENTAL DETAILS

This experiment transmits modulated known random data through a configured Li-ion battery pack, and then receives and demodulates this data. The data sent and the data received are then compared to obtain the bit error rate (BER) and the symbol error rate (SER). In addition, the received QAM constellation is evaluated to calculate the error vector magnitude (EVM) of the communication system tested.

To modulate, demodulate, transmit and receive data, a National Instruments PXIe-5840 vector signal transceiver (VST) is used. The VST is given a known data set of 100,000 random symbols to modulate in the QAM orders of 4, 16, 32, 64, 128, 256, 512, and 1024-QAM. This data set starts with a custom sequence of training symbols, which is a repetition of all possible symbols in each QAM-constellation. This allows
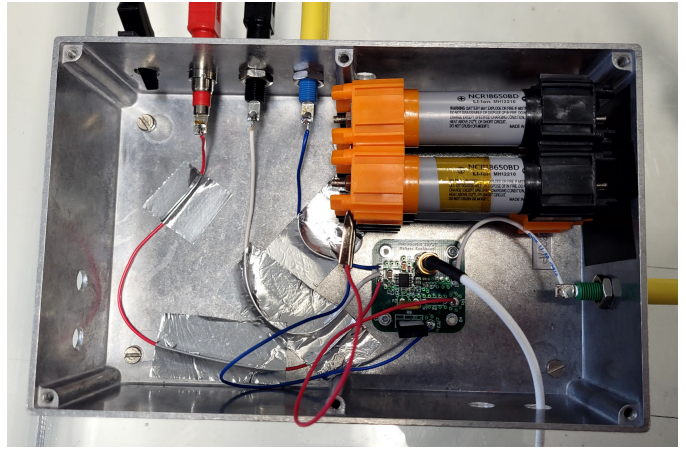

Fig. 1. Photo of the DC offset circuit and the battery pack under test within a Faraday shield (with top lid removed).
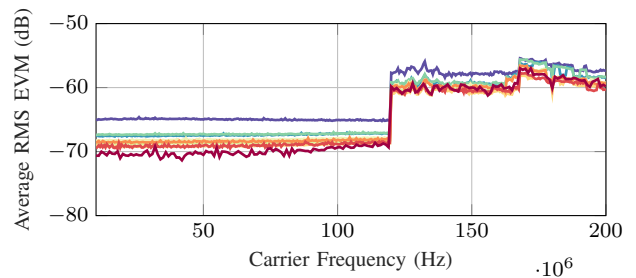

Fig. 2. Average RMS EVM for various QAM-signals with the transmitter and the receiver directly connected.

for the VST to perform phase shift compensation and auto-gain filtering on the receiver. These signal filtering techniques are commonplace within QAM demodulators. The higher the QAM order, the more bits per symbol are transmitted. Hence, whereas the number of symbols remain constant for all QAM orders tested, the number of bits that are transmitted within a single test will increase with the QAM order. This will be taken into account in the analysis.

The modulated data is transmitted at carrier frequencies between 10 MHz and 200 MHz, with a step of 500 kHz and a symbol rate of 100 kHz, to a DC offset circuit. This circuit uses a very high speed operational amplifier to apply a DC offset to the transmitted signal. This offset is programmed to counter the voltage produced by the connected Li-ion cells, and protects the receiver of the VST from voltages that exceed its absolute maximum rating. This DC offset circuit provides the same effect as capacitively coupling the output signal of the Li-ion cell. The DC-offset modulated signal is transmitted through the Li-ion battery pack that is configured in one cell, two cells in series (2S), two cells in parallel (2P), and two cells in series and two in parallel (2S2P).

The negative terminal of the battery pack is connected both to a $1\,\Omega$ thick-film, non-inductive resistor to ground, and also to the receiver of the VST. The receiver performs oversampling of eight times the symbol rate, and the output signal produced is
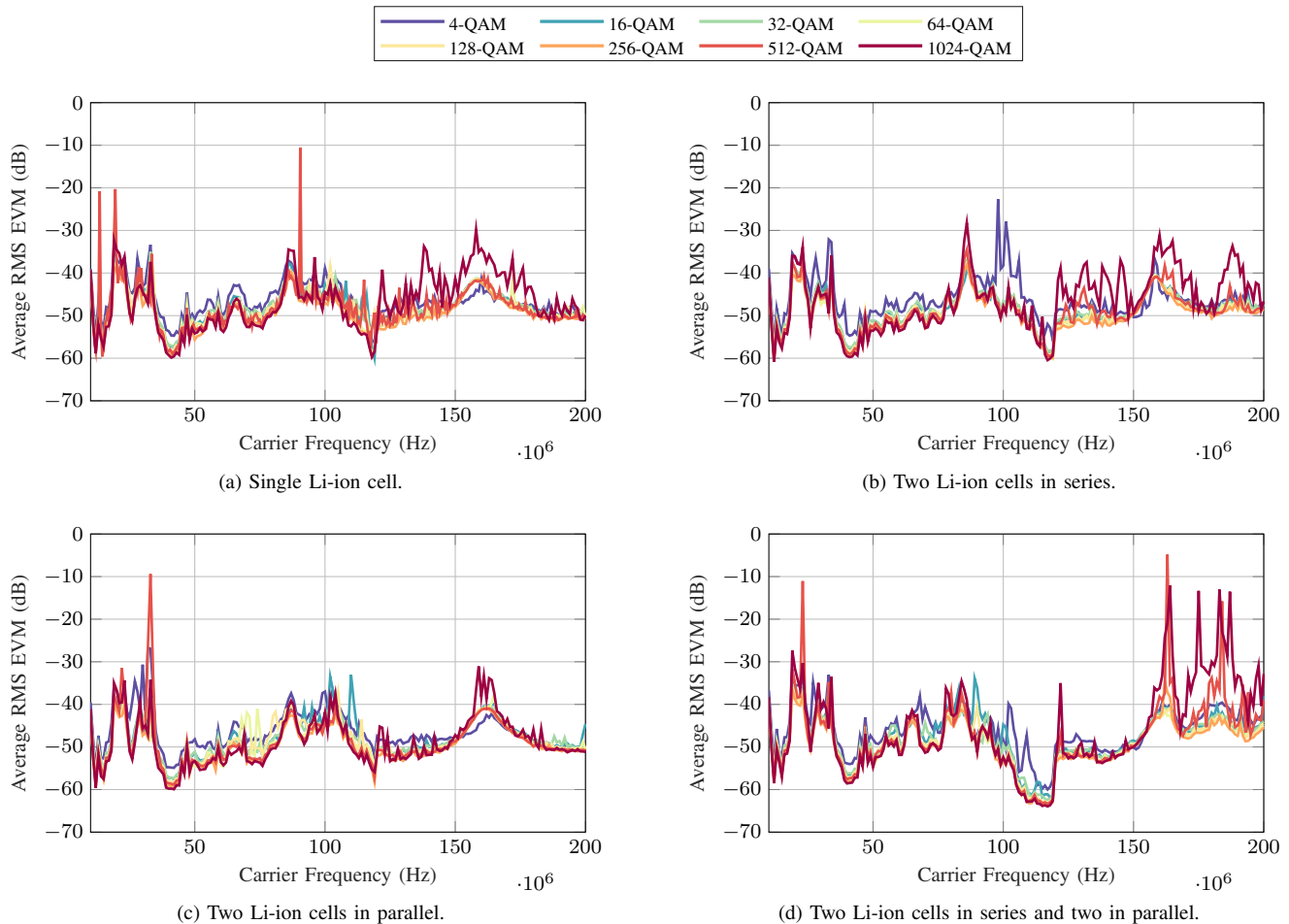
Fig. 3. Average RMS EVM for various QAM-signals transmitted through Li-ion cells.

(a) Single Li-ion cell.

(b) Two Li-ion cells in series.

(c) Two Li-ion cells in parallel.

(d) Two Li-ion cells in series and two in parallel.

an average of each received symbol. Hence, the EVM presented within section III is described as an average.

The measured constellation of the received signal is compared to the reference QAM symbol map, and an EVM is calculated based upon the magnitude of the deviations. This signal is then demodulated to data bits and compared to the data transmitted to obtain the BER and SER. The BER is a ratio of erroneous bits due to the communication channel, and the SER is a ratio of erroneous symbols, which are formed of a specific number of bits dependant on the QAM order. In this experiment, the EVM, BER, and SER will show the impact that the Li-ion battery pack has on the communication system.

To reduce the effects of electromagnetic interference on these results, the DC-offset circuit and the battery pack under test are placed within a Faraday shield, as shown in figure 1.

III. RESULTS AND DISCUSSION

A. EVM

First, the transmitter and the receiver are directly connected together, and the EVM calculated forms a baseline of the lowest possible error that is possible on the communication system. figure 2 shows the EVM in decibel for the carrier frequencies

tested. It can be seen that the EVM remains below −65 dB up to a carrier frequency of 120 MHz, and above 120 MHz the EVM rises to a maximum of −55 dB. This increase in EVM is attributed to the characteristics of the VST whereby for carrier frequencies above 120 MHz, a "LO driven mixing stage" is added to the RF signal path [17].

The average RMS EVM for a single Li-ion cell within the battery pack is shown in figure 3a. It can be observed that the EVM changes with carrier frequency, whereby for 16-QAM the lowest EVM values of −57 dB and −59 dB occur at 41.5 MHz and 118 MHz, respectively. Furthermore, 512-QAM displays the highest peak EVM, occurring at 13.5 MHz and 19.5 MHz, and reaching −10.5 dB at 90 MHz. 4-QAM results in higher EVM than other modulation orders below 120 MHz, whereas up to 200 MHz the EVM of 1024-QAM rises significantly and remains higher than other modulation orders. Whilst 4-QAM may have a relatively high EVM, the significance of this is small in comparison to the EVM of a higher modulation order, such as 1024-QAM. This is because 4-QAM uses only four QAM symbols on the constellation map, in comparison to 1024-QAM which uses 1024 symbols within the same constellation space. Therefore, 4-QAM is relatively

(a) Single Li-ion cell.

(b) Two Li-ion cells in series.

(c) Two Li-ion cells in parallel.

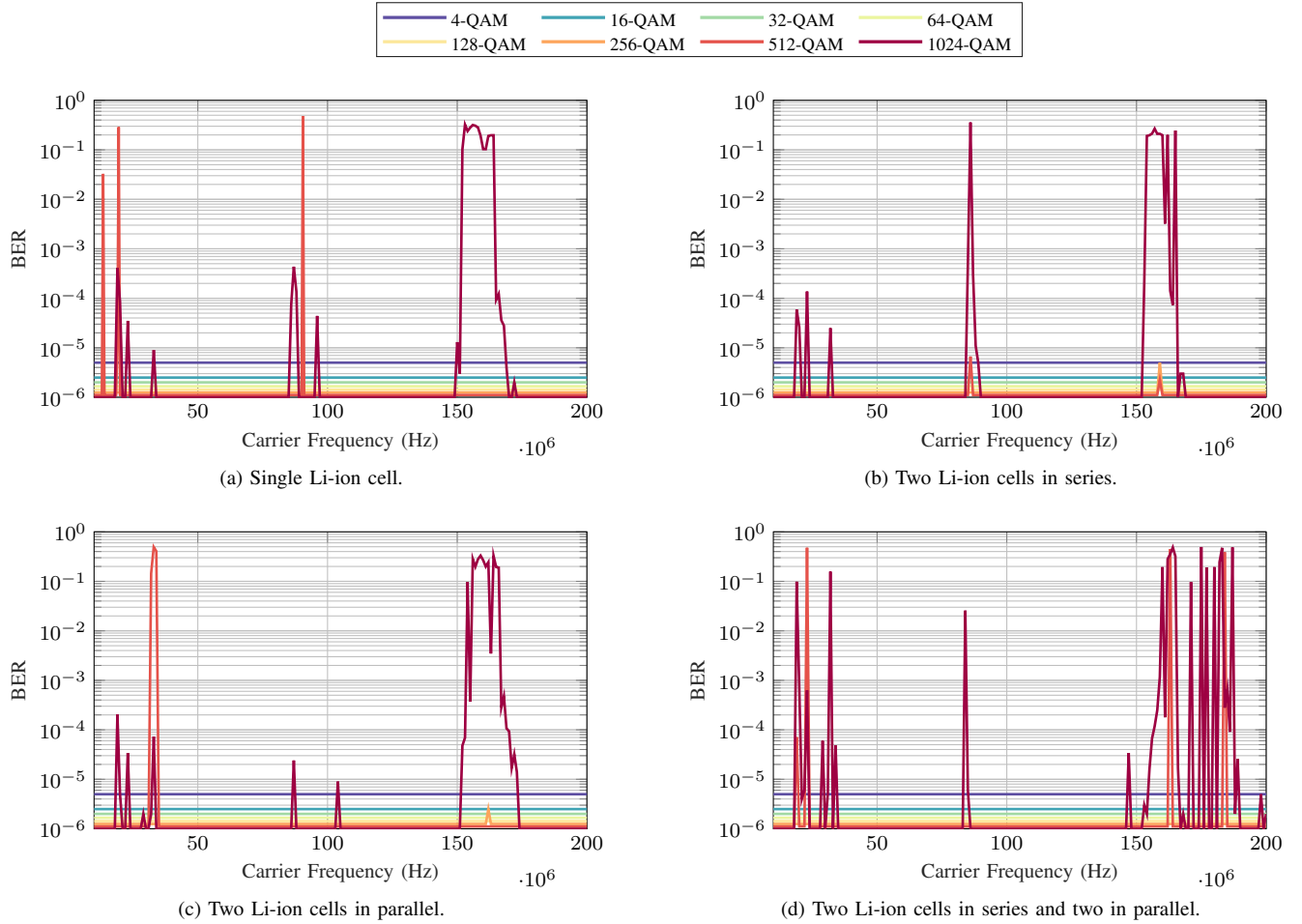(d) Two Li-ion cells in series and two in parallel.

Fig. 4. BER for various QAM-signals transmitted through Li-ion cells.

less susceptible to noise than higher modulation orders. EVM thresholds described within existing communication system standards such as *IEEE 802.11ax* emphasise that higher QAM orders require a lower EVM threshold, such as −13 dB and −35 dB for 4-QAM and 1024-QAM, respectively [18].

Figures 3b and 3c present the EVM for two Li-ion cells in series and parallel, respectively. These figures show that the effects of these Li-ion battery configurations on the communication system are similar to that when only a single Li-ion cell exists within the battery pack. Figure 3b displays that the EVM for 4-QAM rises to a peak of −22.7 dB at 98 MHz, before subsiding to similar EVM values of the higher modulation orders. 1024-QAM results in the highest EVM above 120 MHz for both 2S and 2P configurations.

The results for two Li-ion cells in series and two in parallel in figure 3d present both increases and decreases in EVM in comparison to the other battery configurations tested. Between 100 MHz and 120 MHz, the EVM is smaller for all modulation orders, and the frequency range over which this reduction occurs is much wider than in the other battery configurations. Contrasting with the other cell configurations, it also displays a sharp decrease in EVM at 115 MHz rather than a gradual

one. In addition, a sharper and substantial rise in EVM can be seen for 512-QAM and 1024-QAM orders above 155 MHz, with the most significant peak EVM reaching −4.8 dB.

These results thus far demonstrate that not only does the Li-ion cell affect the performance of in-situ PLC, the configuration of the cells can offer a significant negative or positive impact on the communication channel depending on the carrier frequency selected. The reduced EVM between 110 MHz and 120 MHz may be attributed to the changes in reactance and internal resistance of the cells, whereby simulations of in-situ Li-ion cell PLC performance utilising real electrochemical impedance spectroscopy data demonstrate significant changes in reactance at the same frequencies [13].

B. BER

Figure 4 shows the BER for the four battery configurations tested. Since the number of symbols is kept constant for each QAM order tested, the number of bits measured increases with QAM order. Hence, the horizontal lines indicate that the minimum possible BER for 4-QAM (5×10^{-6}) is higher than the minimum possible for 1024-QAM (1×10^{-6}).
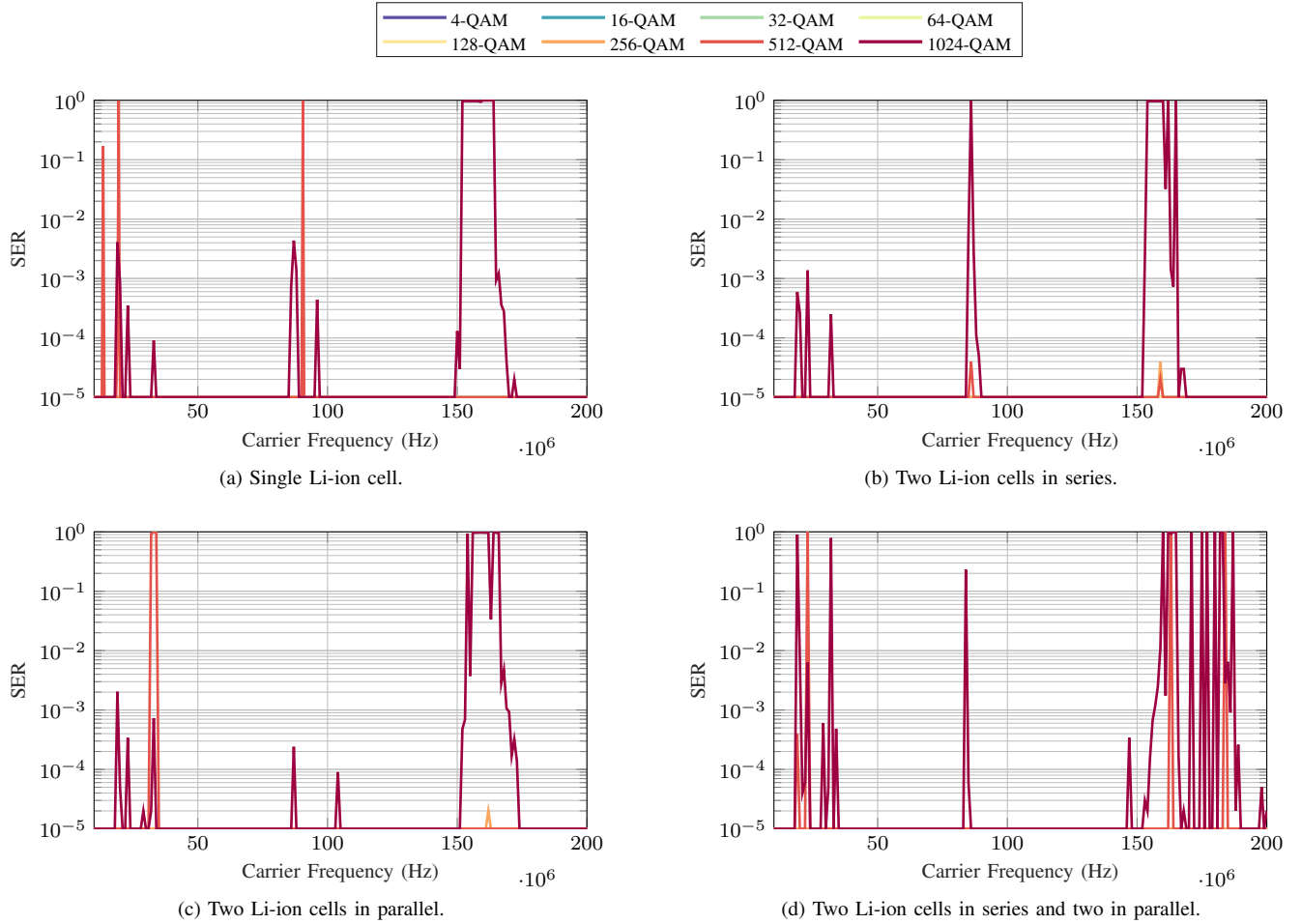
Fig. 5. SER for various QAM-signals transmitted through Li-ion cells.

It can be seen that the error magnitudes correspond with the EVM. For instance, at 160 MHz the increase in EVM corresponds with an increase in BER for 1024-QAM in all battery configurations. Furthermore, the EVM peaks for the single cell configuration for 512-QAM are also seen at the same carrier frequencies in the BER, where the highest value of 0.48 is obtained. In addition, 1024-QAM produces a high BER for the widest carrier frequency range of 152 MHz to 168 MHz for all four battery configurations. In the 2S2P configuration however, the BER for 1024-QAM fluctuates rapidly over this frequency range. This corresponds with the same intense fluctuations in EVM in figure 3d, and shows that the receiver is unable to decode the correct bits once the EVM rises above approximately −35 dB.

For most cell configurations and carrier frequencies, only 512- and 1024-QAM result in a BER higher than the minimum. However, in the 2S and 2P configurations, 256-QAM also shows a small increase in BER at 159 MHz of 5×10^{-6}.

C. SER

Figure 5 presents the SER for the four battery configurations tested. It can be observed that for the same frequencies that

cause high BER, the SER increases too, sometimes even up to 1. In cases where the SER is 1, the effect of the Li-ion on the communication channel is so significant, that the phase shift compensation and the auto-gain filtering of the receiver is not able to demodulate the signal correctly. Between 152 MHz and 168 MHz, the corruption of data is so significant for 1024-QAM that the training symbols are also corrupted, thereby preventing the demodulator from restoring the correct symbol map in all four battery configurations. This effect can also be observed at fewer, specific frequencies with 512-QAM using the 2S2P battery configuration.

From these results, it is inferred that as the number of cells within the battery pack configuration increases, the magnitude of error also increases. Whereas the SER and BER of the 2S and 2P configured communication system are similar, they are slightly higher than those of the single cell configuration. Furthermore, the BER and SER of the 2S2P configuration is higher for a larger range of carrier frequencies. In contrast, the 2S2P configuration shows reduced BER and SER in comparison to the other battery pack configurations within a small range of carrier frequencies, such as 173 MHz.

Modulation orders of 256-QAM and below do not deviate

from the minimum possible BER and SER values. This suggests that for these battery configurations, any carrier frequency may be used. However, the noise of the target system, which for BEVs includes DC-DC switching noise, must be considered. It is therefore appropriate to take into account carrier frequencies that display reduced EVM. Therefore, it can be concluded that acceptable carrier frequencies for the battery pack configurations tested are in the ranges of 40 MHz to 80 MHz, and 105 MHz to 148 MHz. At these frequencies, all QAM orders tested show minimum BER and SER, and the EVM recorded is at its lowest. Carrier frequencies within this range will be less susceptible to noise on the communication channel. However, changes to the battery pack configuration, such as the addition of cells, changes to state of charge, or changes to state of health, may change the reactance and resistance of the cells, which as a consequence may attenuate or phase shift the signal. In this case, it is recommended to reduce the QAM order to reduce the effect of noise on the QAM symbol map.

IV. CONCLUSIONS

In this paper, four distinct battery pack configurations of 18650-model Li-ion cylindrical cells have been tested for their effect on an in-situ power line communication (PLC) system that utilises quadrature amplitude modulation for carrier frequencies of 10 MHz to 200 MHz.

The error vector magnitude, bit error rate, and symbol error rate show that the configuration of the Li-ion cells and the carrier frequencies have distinct effects on the communication channel. With higher QAM-orders, the use of carrier frequencies between 152 MHz and 168 MHz results in significant data corruption. Improved error rates are observed at carrier frequencies between 105 MHz to 148 MHz, which corresponds with established research that demonstrates low error rates at these frequencies based upon simulations that utilise real Li-ion electrochemical impedance spectroscopy data [13].

Based upon these findings, it is concluded that carrier frequencies within the ranges of 40 MHz to 80 MHz, and 105 MHz to 148 MHz, show higher resilience against noise. Furthermore, whereas the highest QAM order tested is able to send the largest number of bits within a symbol, it is recommended that a lower QAM order is used for PLC systems targeting an electric vehicle battery pack. This is because of additional noise on the communication channel within a battery electric vehicle energy storage system, including DC-DC switching noise, that is expected to be large enough to produce errors on the highest QAM order communication system. This work has shown that the signal quality of PLC strongly depends on the configuration of Li-ion cells within a battery pack, the carrier frequency and the modulation order. Therefore, appropriate parameters must be selected to ensure optimal performance for a PLC system within a large-scale energy storage system and a smart grid. Ongoing work includes performance analysis of PLC when used within Li-ion batteries under various state of charge and state of health conditions.

REFERENCES

[1] H. He, D. Liu, X. Lu, and J. Xu, "ECO driving control for intelligent electric vehicle with real-time energy," *Electronics*, vol. 10, no. 21, p. 2613, Oct. 2021.

[2] B. Lebrouhi, Y. Khattari, B. Lamrani, M. Maaroufi, Y. Zeraouli, and T. Kousksou, "Key challenges for a large-scale development of battery electric vehicles: A comprehensive review," *Journal of Energy Storage*, vol. 44, p. 103273, Dec. 2021.

[3] D. Andrea, *Battery Management Systems for Large Lithium Battery Packs*. Artech House Publishers, Sep. 2010.

[4] F. Arshad, J. Lin, N. Manurkar, E. Fan, A. Ahmad, M. un Nisa Tariq, F. Wu, R. Chen, and L. Li, "Life cycle assessment of lithium-ion batteries: A critical review," *Resources, Conservation and Recycling*, vol. 180, p. 106164, May 2022.

[5] J. Fleming, T. Amietszajew, J. Charmet, A. J. Roberts, D. Greenwood, and R. Bhagat, "The design and impact of in-situ and operando thermal sensing for smart energy storage," *Journal of Energy Storage*, vol. 22, pp. 36–43, Apr. 2019.

[6] A. P. Talei, W. A. Pribyl, and G. Hofer, "Considerations for a power line communication system for traction batteries," *e & i Elektrotechnik und Informationstechnik*, vol. 138, no. 1, pp. 3–14, Jan. 2021.

[7] R. Zhang, J. Wu, R. Wang, R. Yan, Y. Zhu, and X. He, "A novel battery management system architecture based on an isolated power/data multiplexing transmission bus," *IEEE Transactions on Industrial Electronics*, vol. 66, no. 8, pp. 5979–5991, Aug. 2019.

[8] G. Zhang, S. Ge, T. Xu, X.-G. Yang, H. Tian, and C.-Y. Wang, "Rapid self-heating and internal temperature sensing of lithium-ion batteries at low temperatures," *Electrochimica Acta*, vol. 218, pp. 149–155, Nov. 2016.

[9] D. F. Frost and D. A. Howey, "Completely decentralized active balancing battery management system," *IEEE Transactions on Power Electronics*, vol. 33, no. 1, pp. 729–738, Jan. 2018.

[10] S. Huang, X. Wu, G. M. Cavalheiro, X. Du, B. Liu, Z. Du, and G. Zhang, "In situ measurement of lithium-ion cell internal temperatures during extreme fast charging," *Journal of The Electrochemical Society*, vol. 166, no. 14, pp. A3254–A3259, 2019.

[11] E. Hosseinzadeh, R. Genieser, D. Worwood, A. Barai, J. Marco, and P. Jennings, "A systematic approach for electrochemical-thermal modelling of a large format lithium-ion battery for electric vehicle application," *Journal of Power Sources*, vol. 382, pp. 77–94, Apr. 2018.

[12] I. Ouannes, P. Nickel, and K. Dostert, "Cell-wise monitoring of lithium-ion batteries for automotive traction applications by using power line communication: battery modeling and channel characterization," in *18th IEEE International Symposium on Power Line Communications and Its Applications*. IEEE, Mar. 2014, pp. 24–29.

[13] M. J. Koshkouei, E. Kampert, A. D. Moore, and M. D. Higgins, "Evaluation of an in situ QAM-based power line communication system for lithium-ion batteries," *IET Electrical Systems in Transportation*, Jun. 2021.

[14] T. A. Vincent, B. Gulsoy, J. E. H. Sansom, and J. Marco, "A smart cell monitoring system based on power line communication—optimization of instrumentation and acquisition for smart battery management," *IEEE Access*, vol. 9, pp. 161 773–161 793, 2021.

[15] M. J. Koshkouei, E. Kampert, A. D. Moore, and M. D. Higgins, "Impact of lithium-ion battery state of charge on in-situ QAM-based power line communication," *Sensors*, Aug. 2022.

[16] H. Rahimi-Eichi, U. Ojha, F. Baronti, and M.-Y. Chow, "Battery management system: An overview of its application in the smart grid and electric vehicles," *IEEE Industrial Electronics Magazine*, vol. 7, no. 2, pp. 4–16, Jun. 2013.

[17] National Instruments. (2022, Jan.) Interconnecting multiple pxie-5840 rf channels (homogeneous channel types). [Online]. Available: https://zone.ni.com/reference/en-XX/help/373680F-01/vstdevices/interconnecting_multiple_5840_rf_channels/

[18] IEEE, "IEEE standard for information technology–telecommunications and information exchange between systems - local and metropolitan area networks–specific requirements - part 11: Wireless LAN medium access control (MAC) and physical layer (PHY) specifications," *IEEE Std. 802.11-2020*, Feb. 2021.